Cobalt(II) and cobalt(III) complexes of tripodal tetradentate diamino-bis(phenolate) ligands: Synthesis, characterization, crystal structures and evaluation in radical polymerization processes

Maxime Michelas, Yasmine Redjel, Jean-Claude Daran, Meriem Benslimane, Rinaldo Poli, Christophe Fliedel

Cobalt(II) and cobalt(III) complexes of tripodal tetradentate diamino-bis(phenolate) ligands: Synthesis, characterization, crystal structures and evaluation in radical polymerization processes

Maxime Michelas,[a] Yasmine K. Redjel,[a,b] Jean-Claude Daran,[a] Meriem Benslimane,[b] Rinaldo Poli[a,c] and Christophe Fliedel[a,*]

[a] Laboratoire de Chimie de Coordination (LCC-CNRS), Université de Toulouse, CNRS, INPT, Toulouse, France

[b] Unité de Recherche de Chimie de l'Environnement et Moléculaire Structurale, Faculté des Sciences Exactes, Département de Chimie, Université de Constantine 1, 25000 Constantine, Algeria

[c] Institut Universitaire de France, 1 rue Descartes, 75231 Paris, Cedex 05, France

* Corresponding author. E-mail address: christophe.fliedel@lcc-toulouse.fr (C. Fliedel)

Keywords:

Amino-phenolate ligands – Cobalt – X-ray crystallography – Acetato (OAc) complex – Radical polymerization

Dedicated to Guido Pampaloni on the occasion of his retirement.

Abstract

The synthesis and characterization of cobalt(II) (**3**, **4**) and acetato cobalt(III) (**5**) complexes with two tripodal tetradentate diamino-bis(phenolate) ligands (**L1** and **L2**) are reported. The solid-state structures of proligand H_2**L1** and complexes **4** and **5** were determined by X-ray crystallography. Complex **4** crystallizes as a dimer *via* the formation of a Co_2O_2 core. Complex **5** is monomeric with a six-coordinated cobalt(III) center bearing a chelating acetate ligand. In both structures, the diamino-bis(phenolate) ligand (**L1** or **L2**) is acting as a tetradentate dianionic κ^4-(O_2,N_2) chelating ligand. The diamagnetic nature of complex **5** allowed its characterization by multinuclear NMR spectroscopic techniques. Complex **5** is not a competent unimolecular initiator for the radical polymerization of methyl acrylate or methyl methacrylate. Its cobalt(II) analog (**3**) did not act as an efficient OMRP moderator for the radical polymerization of activated (styrene, *tert*-butyl acrylate) and non-activated (vinyl acetate) monomers.

1. Introduction

Cobalt is an essential physiological element (vitamin B_{12} and other enzymes) that is found only in low abundance in the Earth's crust and its complexes have found many applications in diverse fields of chemistry, such as biomedical areas (imaging, anticancer/antitumor therapy or as antiviral and antibacterial agents) [1-3], materials (*e.g.* single-molecule magnets [4, 5] and lithium-ion batteries [6]), and catalysis (hydrogenation, cross-coupling, hydrofunctionalization, cycloaddition, water oxidation, *etc.*) [7-11]. Polymerization is another important area in which cobalt complexes have proven to be very efficient. This includes diverse sub-areas such as coordination/insertion (living) ethylene polymerization [12], (stereoselective) ring-opening polymerization of epoxides or copolymerization of epoxides and carbon dioxide [13-15], and controlled radical polymerization by the organometallic approach (organometallic-mediated radical polymerization or OMRP)[13, 16-21]. For the latter applications, the use of Schiff-bases as supporting ligands for the Co ion has long been predominant [14, 22-24]. However, the use of other ligand scaffolds, particularly those incorporating amino-phenolate moieties, led to efficient systems for the copolymerization of epoxides and CO_2 [25-27].

Our group is especially interested in metal-mediated radical polymerizations such as atom transfer radical polymerization (ATRP) [28, 29] and OMRP [21, 30] and in the study of interfering reactions and their mechanisms [31-36]. Both ATRP and OMRP techniques belong to the family of reversible-deactivation radical polymerization (RDRP) techniques [37, 38]. These techniques control radical polymerization processes by establishing a dynamic equilibrium between the active/propagating radical species ($P_{n/m}^{\bullet}$) and a dormant species ($P_{n/m}$-Y), the latter resulting from the quenching of the radical by a moderator (Y), which favors the controlled polymeric chain growth versus bimolecular radical terminations (coupling and disproportionation). Scheme 1 (bottom) shows the dynamic equilibrium under reversible-termination (RT) and degenerative transfer (DT) modes for the specific case of OMRP, *i.e*. Y = L/Mt. Copper-mediated ATRP is now commonly applied in academic laboratories and in several industrial processes [39, 40], allows the preparation of advanced materials [41] and can be initiated in a variety of ways such as “normal”, “reverse”, “AGET” and “SARA” [42], and run under various conditions (*e.g*. photo- or electronically induced, ppm levels of catalysts, aerobic conditions, *etc.*) [13, 42, 43]. In contrast, OMRP is much less investigated, but proved very efficient for the controlled (co)polymerization of so-called less-stabilized monomers (LAMs) such as vinyl acetate [44], vinyl chloride [45] and vinylidene fluoride [16, 17, 46], especially when using cobalt complexes as moderators [47]. In OMRP, “direct” and “reverse” initiation paths can be distinguished [13]. A direct initiation occurs *via* homolysis of a [L/Mt^{x+1}-R_0’] organometallic species, furnishing the primary radical $^{\bullet}R_0$’ and the [L/Mt^{x}] moderator. In contrast, a reverse initiation requires the use of a radical precursor, typically an azo-compound such as AIBN [2,2’-azobis(2-methylpropionitrile)], to generate the primary radical (R_0) and the presence of the moderator (Scheme 1). While the reverse initiation necessitates the use of sensitive radical initiators and a suitable [L/Mt^{x}] complex, which is often subject to easy oxidation, the direct initiation appears more attractive. However, only very few unimolecular systems were reported; they are not easily accessible and are generally sensitive to heat or light [48-51].

We are currently working on the development of air-stable and easy-to-handle unimolecular [L/Mt-R_0] OMRP initiators to offer an alternative to the existing systems [48, 52, 53], with a special emphasis on cobalt-based systems due to their excellent performances in OMRP. In the present contribution, we report the synthesis of cobalt(III) carboxylate complexes of diamino bis-phenolate ligands, which were chosen on the basis of a recent work showing the ability of their iron(III) halide analogues to moderate the radical polymerization of styrene and methyl methacrylate under a cooperative ATRP/OMRP mechanism [54]. Cobalt(II) counter parts were also synthesized and tested as potential moderators for processes with reverse initiation.

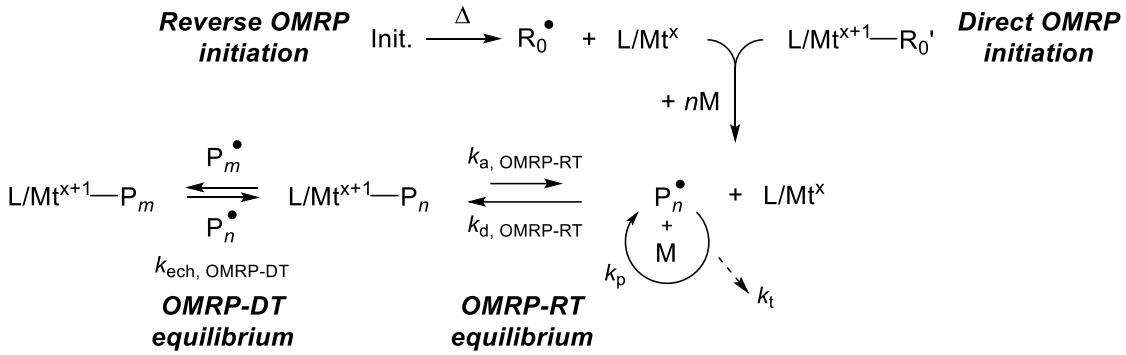

Scheme 1. Direct and reverse initiation mechanisms (top) and control equilibria (bottom) of an organometallic-mediated radical polymerization (OMRP) process.

2. Experimental part

2.1. General considerations

The syntheses of the cobalt(II) complexes and the polymerization tests were conducted under an inert atmosphere (Ar), using standard Schlenk techniques or in an argon-filled glovebox, in flame-dried glassware and with dried and/or distilled monomers and solvents (see below). All other operations were carried out in air and using non-dried glassware and solvents.

2.2. Materials

Compounds cobalt(II) acetate (Sigma Aldrich, 99.99%), cobalt(II) acetylacetonate (Acros Organics, 99%), potassium hydroxide (Fisher Chemical, analytical reagent grade), triethylamine (Acros Organics, 99%), 2,2'-azobis(2-methylpropionitrile) (AIBN, Sigma Aldrich, 98%), 2,2'-Azobis(4-methoxy-2,4-dimethylvaleronitrile) (V-70, Wako Chemicals), 1,3,5-trioxane (Sigma Aldrich, ≥99%) were used as received. Methyl methacrylate (MMA, Sigma Aldrich, 99%), methyl acrylate (MA, Acros Organics, 99%), styrene (St, Sigma Aldrich, ≥99%), vinyl acetate (VAc, Acros Organics, 99%) and *tert*-butyl acrylate (*t*BA, Sigma Aldrich, 98%) were passed through a column filled with neutral alumina, dried over calcium hydride (CaH_2), distilled under reduced pressure, degassed by several freeze/pump/thaw cycles and stored in a freezer under argon. Anhydrous methanol and chloroform (≥99%, Sigma Aldrich), reagent grade pentane (≥99.5%, VWR Chemicals) and $CDCl_3$ (99.8%D, Euriso-top) were used as received, without prior purification. Toluene was dried using an MBraun SPS system. Ligands H_2**L1** [55] and H_2**L2** [56] were prepared according to literature methods.

2.3. Instrumentation

The NMR spectra were recorded on a Bruker Avance III 300 or 400 MHz spectrometer at ambient temperature. ^{1}H and ^{13}C chemical shifts (δ) are reported in ppm *vs*. $SiMe_4$ and were determined using the residual ^{1}H and ^{13}C solvent peaks as internal standards. The coupling constants are reported in Hertz. The IR spectra were recorded in the 4000−100 cm^{-1} region on a PerkinElmer Frontier FT-IR spectrometer (ATR mode, diamond crystal). The electrospray ionization mass spectra (ESI-MS) were recorded on a Q-Tof Premier (Waters) instrument using nitrogen as drying agent and nebulizing gas and MeCN as solvent. The elemental analyses for all compounds were carried out by the analytical service of the LCC-Toulouse using a PerkinElmer 2400 CHNS/O Series II System (100V). The M_n and M_w/M_n of the polymers were determined by gel permeation chromatography (GPC) using a Shimadzu system equipped with a Shimadzu RID-20A refractive index detector and with two polymer standards service SDV analytical columns (1000 and 100 000 Å, 5 µm, 8 × 300 mm). Tetrahydrofuran (THF) was used as the eluent at a flow rate of 1 mL min^{-1} at 35 °C. Linear polystyrene standards were used for calibration.

2.4. X-ray structural analyses

A single crystal of each compound was mounted under inert perfluoropolyether at the tip of a glass fiber and cooled in the cryostream of either a Rigaku Oxford-Diffraction XCALIBUR Gemini EOS diffractometer for H_2**L1**, a Nonius Bruker APEXII diffractometer for **4**·$CHCl_3$ and a Bruker APEXII for **5**.

The structures were solved by using the integrated space-group and crystal structure determination SHELXT software [57] and refined by least-squares procedures on F^2 using SHELXL-2014 [58]. All H atoms attached to carbon or oxygen atoms were introduced in the calculations at idealised positions and treated according to the riding model. Compound **4**·$CHCl_3$ is a dinuclear complex arranged around an inversion centre, with half a molecule within the asymmetric unit. The two *tert*-butyl groups (C18 and C28) are statistically disordered. These disorders were treated using the tools (PART and SAME) available in SHELXL-2014. In compound **5**, some residual electron density was difficult to model and therefore, the SQUEEZE function of PLATON [59] was used to eliminate the contribution of the electron density in the solvent region from the intensity data and the solvent-free model was employed from the final refinement. There are two cavities of 359 Å^3 per unit cell. PLATON estimated that each cavity contains 102 electrons which may correspond to a mixture of pentane and chloroform solvent molecules as suggested by chemical analyses. Crystal data and refinement parameters are shown in Table 1.

2.5. Synthesis of complex [Co^{II}(**L1**)] (**3**)

In an argon-filled glovebox, solid [$Co(acac)_2$] (944 mg, 3.7 mmol) was added in one portion to a solution of pro-ligand H_2**L1** (2 g, 3.7 mmol) and KOH (412 mg, 7.4 mmol) in a 1:1 mixture of dry MeOH/$CHCl_3$ (50 mL) at room temperature. The resulting mixture was kept under inert atmosphere and refluxed with stirring for 18 h. The resulting purple suspension was filtered through a Celite pad and the volatiles were removed under reduced pressure. The crude product was washed with pentane (2 x 20 mL) and dried under vacuum, leading to complex **3** as a light purple powder (1.96 g, 88%). Anal. Calcd. for $C_{36}H_{50}CoN_2O_2$ (601.74): C, 71.86; H, 8.38; N, 4.66. Found: 71.33; H, 8.46; N, 4.60. FTIR: ν_{max}(solid)/cm^{-1}: 2953br, 1579vs, 1516vs, 1460s, 1398vs, 1357s, 1317m, 1276w, 1256s, 1201w, 1169w, 1017m, 923m, 877w, 762s, 650m, 552s, 449s, 422m. MS (ESI): m/z 601.3 [M]$^+$. UV-Vis: λ_{max}(toluene)/nm: 506 (ε/dm^3 mol^{-1} cm^{-1}: 0.19); 529 (ε/dm^3 mol^{-1} cm^{-1}: 0.17).

The same reaction was carried out with [$Co(OAc)_2$] (650 mg, 3.7 mmol) instead of [$Co(acac)_2$], leading to complex **3** in 83% yield (1.85 g).

2.6. Synthesis of complex [Co^{II}(**L2**)] (4)

The same procedure as for **3** was applied, starting from [$Co(OAc)_2$] (830 mg, 4.7 mmol) or [$Co(acac)_2$] (1.21 g, 4.7 mmol), pro-ligand H_2**L2** (2 g, 4.7 mmol) and KOH (526 mg, 9.4 mmol) in 50 mL of dry MeOH/$CHCl_3$ (1:1). Complex **4** was isolated as a pink-purple powder (1.93 g, 85% with [$Co(OAc)_2$]; 1.84 g, 81% with [$Co(acac)_2$]). Suitable crystals for the X-ray diffraction analysis were grown by slow evaporation of a saturated $CHCl_3$ solution of **4** at room temperature over two weeks. Anal. Calcd. for $C_{27}H_{40}CoN_2O_2$ (483.56): C, 67.06; H, 8.34; N, 5.79. Found: 66.76; H, 8.30; N, 5.86. FTIR: ν_{max}(solid)/cm^{-1}: 2952br, 2867sh, 1645w, 1567s, 1557s, 1465vs, 1434s, 1412vs, 1361m, 1303m, 1235s, 1203w, 1165w, 1017w, 1004w, 931w, 875m, 863m, 806m, 761s, 738m, 646s, 624sh, 541m, 481m, 449m. MS (ESI): m/z 483.2 [M]$^+$. UV-Vis: λ_{max}(toluene)/nm: 512 (ε/dm^3 mol^{-1} cm^{-1}: 0.19); 532 (ε/dm^3 mol^{-1} cm^{-1}: 0.21).

2.7. Synthesis of complex [Co^{III}(**L1**)(OAc)] (**5**)

Solid [$Co(OAc)_2$] (32.5 mg, 0.18 mmol) was added in one portion to a solution of pro-ligand H_2**L1** (100 mg, 0.18 mmol) and excess of NEt_3 (0.5 mL) in a 2:1 mixture of MeOH/$CHCl_3$ (30 mL) at room temperature. The resulting mixture was stirred at room temperature in air during 24 h. The crude product obtained after removal of the volatiles was recrystallized from $CHCl_3$, leading to complex **5** as

a dark red powder (75.2 mg, 62%). Suitable crystals for the X-ray diffraction analysis were grown by slow diffusion of pentane into a saturated $CHCl_3$ solution of **5** over a week at room temperature. Anal. Calcd. for $C_{38}H_{53}CoN_2O_4$ (660.79): C, 69.07; H, 8.08; N, 4.24. Found: 68.79; H, 8.30; N, 4.34. FTIR: ν_{max}(solid)/cm^{-1}: 2950br, 1602w, 1515w, 1470vs, 1443s, 1411s, 1361m, 1277s, 1238m, 1203m, 1167m, 1130w, 1059w, 950w, 914w, 875w, 835m, 805w, 763s, 748m, 688vs, 625m, 554m, 496s, 438m. MS (ESI): m/z 601.3 $[M - OAc]^+$. UV-Vis: λ_{max}(toluene)/nm: 428 (ε/dm^3 mol^{-1} cm^{-1}: 2687). ^{1}H NMR (400 MHz, $CDCl_3$): δ (ppm) 8.55 (d, ^3J = 5.7 Hz, 1H, $H_{arom,}$ Py), 7.39 (t, ^3J = 7.7 Hz, 1H, $H_{arom,}$ Py), 6.99 (t, ^3J = 6.7 Hz, 1H, $H_{arom,}$ Py), 6.94 (d, ^4J = 2.5 Hz, 2H, $H_{arom,}$ Phenol), 6.79 (d, ^4J = 2.5 Hz, 2H, $H_{arom,}$ Phenol), 6.63 (d, ^3J = 7.9 Hz, 1H, $H_{arom,}$ Py), 4.59 (d, ^2J = 13.3 Hz, 2H, CH_2), 3.97 (s, 2H, CH_2), 3.06 (d, ^2J = 13.2 Hz, 2H, CH_2), 1.95 (s, 3H, $OC(CH_3)O$), 1.31 (s, 18H, ^{t}Bu), 1.20 (s, 18H, ^{t}Bu). $^{13}C\{^1H\}$ NMR (101 MHz, $CDCl_3$): δ (ppm) 191.75 ($OC(CH_3)O$), 163.28 (C_{quat}), 163.11 (C_{quat}), 151.41 (CH_{arom}, Py), 140.87 (C_{quat}), 138.02 (CH_{arom}, Py), 135.97 (C_{quat}), 123.72 (CH_{arom}, Phenol), 123.48 (CH_{arom}, Phenol), 121.87 (CH_{arom}, Py), 119.57 (C_{quat}), 118.75 (CH_{arom}, Py), 64.69 (NCH_2Phenol), 63.21 (NCH_2Py), 35.53 ($C(CH_3)_3$), 34.03 ($C(CH_3)_3$), 31.87 ($C(CH_3)_3$), 30.06 ($C(CH_3)_3$), 23.97 ($OC(CH_3)O$).

2.8. General procedure for the polymerization tests

For the direct initiation. In the glove box, a tube was charged with complex **5** (5.7 mg, 8.6 µmol), trioxane (*ca.* 5 mg) as internal standard and MA (0.23 mL, 2.6 mmol, 300 eq), and then sealed with a septum. The resulting dark brown mixture was stirred at 60°C over a period of 24 h. The monomer conversion was determined by withdrawing aliquots of the reaction mixture for gravimetric and ^{1}H NMR analyses.

A similar procedure was used for the attempt to polymerize MMA, using the following quantities: complex **5** (11.4 mg, 17.2 µmol, 1 eq), MMA (0.54 mL, 5.1 mmol, 300 eq) and trioxane (*ca.* 5 mg).

For the reverse initiation. In the glove box, a tube was charged with complex **3** (20 mg, 33.2 µmol, 1 eq), AIBN (3.3 mg, 20.0 µmol, 0.6 eq), the monomer (500 eq) and *ca*. 5 mg of trioxane as internal standard. The resulting mixture was stirred for 10 min at room temperature for homogenization and the tube was then immersed in a thermostatic oil bath at 65°C. For the polymerization of St and *t*BA, a hard block of polymer was formed in a few minutes. For VAc, aliquots were withdrawn with a degassed syringe at 0.6, 1, 1.5 and 2 h of reaction time and the monomer conversion was determined by ^{1}H NMR. The resulting residue was diluted with THF and the polymer was precipitated using an excess of pentane and dried under vacuum overnight at 80 °C before GPC characterization.

3. Results and discussion

3.1. Synthesis and characterization of the ligands and complexes

The H_2**L1** and H_2**L2** pro-ligands were synthesized according to previously published procedures by Yamauchi and coworkers [55] and our group [56], respectively (Scheme 2). In our previous contribution, we reported that all attempts to crystalize H_2**L2** failed and we only succeeded in crystallizing its HCl adduct (H_3**L2**$^+Cl^-$) [56]. To date, pro-ligand H_2**L1** was only structurally characterized in its $[CuCl_2]$ [55] and $[Ni(OAc)_2]$ [60] adducts. Along the course of the present work, we succeeded in growing single crystals of H_2**L1**, suitable for X-ray diffraction studies, by slow diffusion of pentane into a saturated dichloromethane solution. Its molecular structure is depicted in Fig. 1. Pro-ligand H_2**L1** crystallized in the $P2_1/c$ space group with four independent molecules in the unit cell. The "central" nitrogen atom (N1), which connects the three arms, has a nearly perfect tetrahedral geometry with the Cx-N1-Cy (x, y = 1, 2, 3) angles ranging between 109.51(8) and 111.46(8)°. Three intramolecular H-bonds are observed (Fig. 1), two of them involving N1 as a proton acceptor towards the O-H groups of both phenol rings (N1···O2 2.7318(13) Å and N1···O3 3.0768(12) Å). The third one connects the pyridine

N16 atom as a proton acceptor and O3-H (2.8637(14) Å). Intramolecular H-bonds between the "central" nitrogen atom and the phenol moieties are regularly observed in the crystal structures of (di)amino bis-phenolate ligands [61-65]. Thus, the O3-H proton donor is involved in bifurcated hydrogen bonding with two proton acceptors.

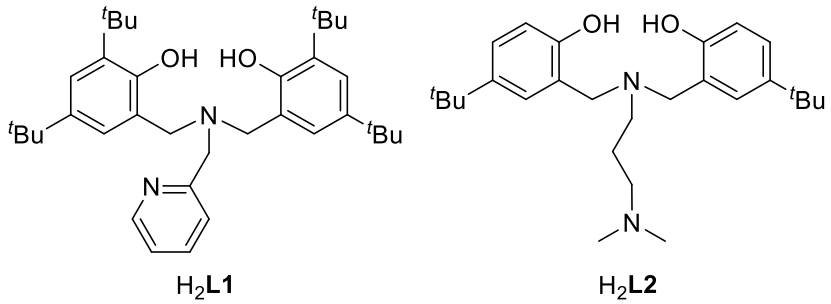

Scheme 2. Pro-ligands H_2**L1** and H_2**L2**.

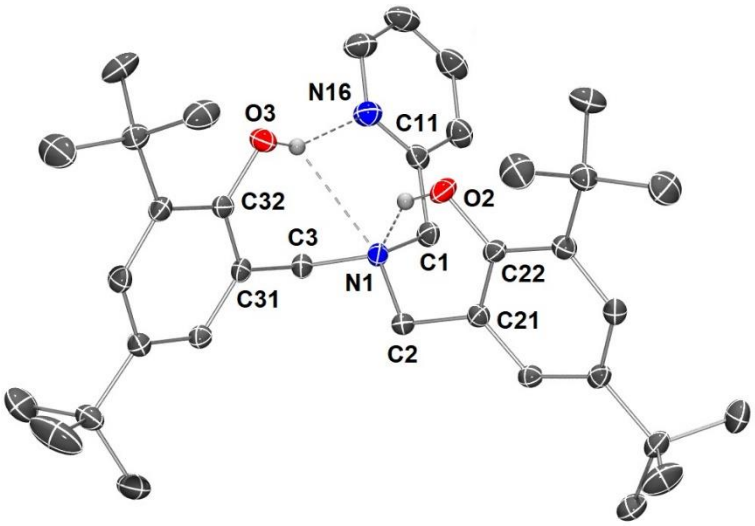

Fig. 1. View of the molecular structure of H_2**L1**. Only the hydrogen atoms of the OH groups are represented for clarity. Ellipsoids are represented at the 50% probability level. Selected bond lengths (Å) and angles (°): N1–C1 1.4624(14), N1–C2 1.4777(13), N1–C3 1.4792(13), C22–O2 1.3730(13), C32–O3 1.3661(13), C1–N1–C2 111.46(8), C1–N1–C3 110.29(9), C2–N1–C3 109.51(8).

In our previous contribution, we have shown that acetylacetonato cobalt(III) and iron(III) complexes of ligands **L1** and **L2**, of general formula [M(acac)(**L**)] (M = Co or Fe; L = **L1** or **L2**), do not behave as unimolecular initiators of a radical polymerization process [56]. Therefore, in the present contribution, we aimed at assessing two points: 1) the behavior of the corresponding cobalt(II) complexes as moderators in OMRP, *via* reverse initiation (see Introduction) and 2) the ability of the corresponding acetato cobalt(III) complexes to initiate a radical polymerization. We focused on cobalt complexes and excluded from this study their iron analogues, because of their generally observed lower performances as moderators in radical polymerization [20, 66].

First, we explored the synthetic pathways to access the cobalt(II) complexes of the diamino bis-phenolate ligands **L1** and **L2**. Our initial attempts, which consisted in reacting the pro-ligands with a base (NEt_3 or KO^tBu) followed by the addition of [$CoCl_2$], or directly in the presence of [$CoCl_2$], were unsuccessful (most of the metal precursor remained unreacted). Therefore, we turned our attention to the use of cobalt precursors incorporating an internal base, such as [$Co(acac)_2$] and [$Co(OAc)_2$] [67]. The first tests, carried out under stoichiometric conditions (without additional base), with both

[Co(acac)$_2$] and [Co(OAc)$_2$], led only to poor yields of the desired products [Co^{II}(**L1**)] (**3**) and [Co^{II}(**L2**)] (**4**). Further tests were performed with the addition of an external base (NEt$_3$ or KOH). While the results with NEt$_3$ were not satisfying, KOH improved the outcome of the reactions. Careful monitoring of the pro-ligand consumption by TLC highlighted that [Co(acac)$_2$] is much more reactive. Optimized yields were obtained using H$_2$**L**:Co(acac)$_2$:KOH 1:1:2 (L = **L1** or **L2**) in a mixture of toluene and methanol (1:1) at reflux for 18 h (Scheme 3). Whatever the nature of the pro-ligand (H$_2$**L1** or H$_2$**L2**), the yields of the reactions were similar (80-90%, see Experimental part). Complexes **3** and **4** were characterized by elemental analysis (EA), infrared (FT-IR) and UV-Vis spectroscopic techniques and mass spectrometry (ESI-MS). For each complex, the most intense peak in the ESI mass spectrum corresponds to [M]$^+$ with the expected isotopic distribution (Figures S1 and S2, ESI). The UV-vis spectra of complexes **3** and **4** (Figure S8, ESI) exhibit two distinct absorption bands at similar wavelengths, *i.e*. 506 and 529 nm for **3** and 512 and 532 nm for **4**, with ε vales in the same order of magnitude (0.17-0.21 dm^3 mol^{-1} cm^{-1}). While all attempts to crystallize complex **3** failed, suitable single crystals of complex **4** for an X-ray diffraction study were grown by slow evaporation from a CHCl$_3$ solution. As shown in Fig. 2, complex **4** crystalizes as a dimer with the two Co(**L2**) units connected *via* two μ-O bridges in a planar Co$_2$O$_2$ central core. The cobalt(II) center is five-coordinated with, as expected, ligand **L2** acting as a tetradentate dianionic κ^4-(O_2,N_2) ligand and the coordination sphere is completed by the coordination of a phenoxy group from the adjacent Co(**L2**) unit, forming the dimeric structure. In this type of five-coordinate metal complexes, the τ parameter allows a quantitative measure of the degree of distortion between the perfect trigonal bipyramid (TBP; τ = 1) and square pyramid (SP; τ = 0) extremes [68, 69]. The value of this parameter for **4** (τ = 0.17) indicates a slightly distorted square pyramidal geometry. The values of the Co-O-Co angles in **4** (101-103°) are quite close to those of the same Co$_2$O$_2$ motif observed in the crystal structures of several other cobalt(II) complexes of diamino-bis(phenolate) ligands [70-74]. However, when sterically demanding groups are present in the *ortho*-positions of the phenolate moieties and/or on the pending N-based donor, preventing the formation of dimeric structures, or upon addition of Lewis bases or in coordinating solvents (L), the corresponding mononuclear [Co(O_2,N_2)(L)] adducts are obtained [75, 76]. Based on the dimeric structure reported for a cobalt(II) complex supported by a ligand analogous to **L1** [75], differing only by the presence of *o*- and *p-tert*-pentyl in place of ^{t}Bu groups, we assume that complex **3** adopts a dimeric structure similar to **4**.

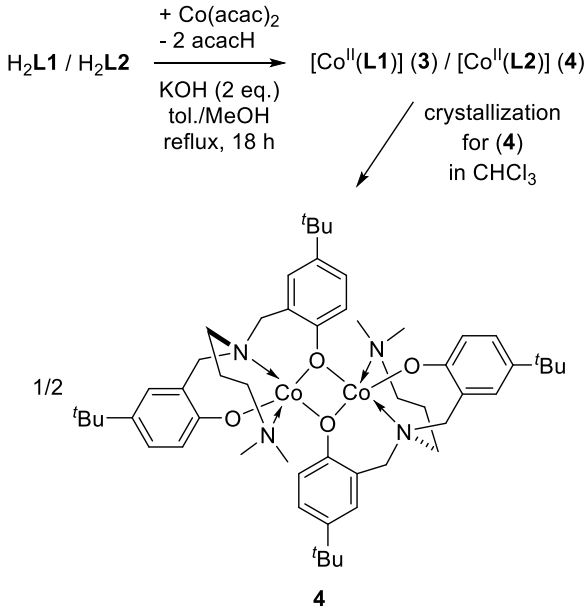

4

Scheme 3. Synthesis of complexes **3** and **4**, and dimeric structure of **4** determined by XRD after crystallization from CHCl$_3$.

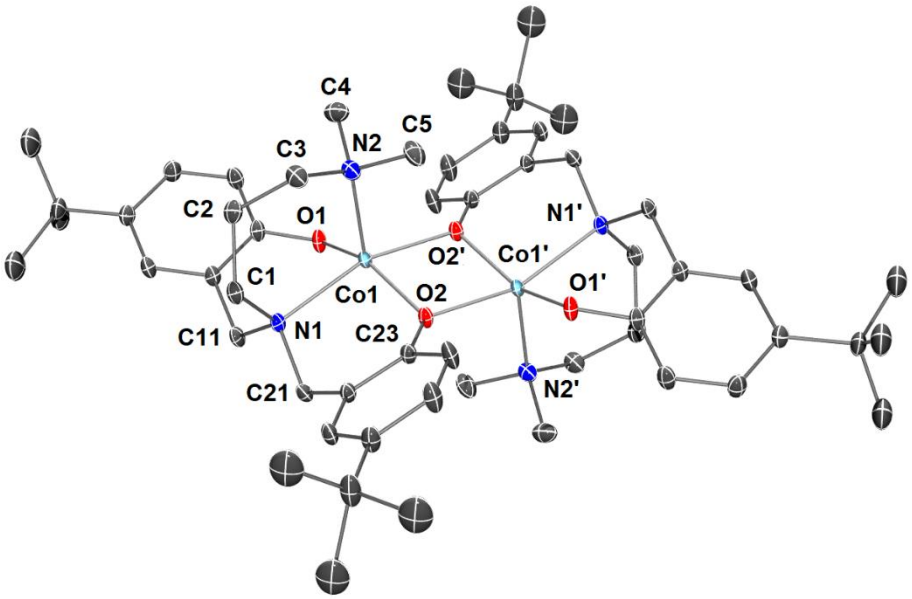

Fig. 2. View of the molecular structure of **4** in **4**·$CHCl_3$. The hydrogen atoms are omitted for clarity. Ellipsoids are represented at the 30% probability level. Selected bond lengths (Å) and angles (°): Co1-O1 1.9313(16), Co1-O2 1.9890(16), Co1-N1 2.2553(19), Co1-N2 2.127(2), Co1-O2' 2.1290(16), N1-Co1-N2 98.19(8), N1-Co1-O1 87.72(7), N1-Co1-O2 90.90(7), N1-Co1-O2' 162.43(7), O1-Co1-O2 152.51(8), Co1-O2-Co1' 101.50(7), C1-N1-C11 109.47(18), C1-N1-C21 110.28(18), C11-N1-C21 104.66(18), C3-N2-C4 110.2(2), C3-N2-C5 107.3(2), C4-N2-C5 108.0(2).

In contrast to the synthesis of the acetylacetonato cobalt(III) complexes with ligands **L1** and **L2** [56], which used the commercially available [Co(acac)$_3$] precursor, the same strategy is not conceivable for the synthesis of the corresponding acetate cobalt(III) complexes, due to non-availability of a [Co(OAc)$_3$] precursor. Other common literature strategies consist of performing the reaction with the cobalt(II) precursor, *i.e.* [Co(OAc)$_2$], under aerobic conditions, which induces the oxidation of the Co^{II} ion to Co^{III}, without formation of any oxo- (from O_2) nor hydroxo- (from H_2O in air) species [76], or of initially oxidizing the metal precursor using H_2O_2 followed by complexation [77]. Given our objective to develop unimolecular initiators for radical polymerization processes, we focused our attention on the complex with the more sterically encumbering ligand, *i.e.* **L1**. Indeed, the [Co^{III}(**L1**)(OAc)] complex (**5**) was obtained in 62% yield after recrystallization, using the first strategy (Scheme 4). Complex **5** is diamagnetic, suggesting an octahedral environment for the Co^{III} metal ion with a d^6 electronic configuration. Its ^1H and $^{13}C\{^1H\}$ NMR spectra (Figures S3-S6, ESI) exhibit all the signals expected for the diamino-bis(phenolate) ligand **L1** [56], and additional resonances for the OAc group, *i.e.* one ^{1} singlet at δ 1.95 ppm (CH_3) [76] and two ^{13}C peaks at δ 24.0 (CH_3) and 191.7 (OCO) ppm. The EA is also in agreement with the [Co(**1**)(OAc)] formula and the ESI-MS spectrum exhibited only one isotopic envelope (with the appropriate distribution) corresponding to the $[M - OAc]^+$ fragment, probably due to the fragility of the Co-OAc bond (Figures S7, ESI). The Co^{III} complex **5** is intensely colored (dark brown), in contrast to its Co^{II} analog (**3**, light purple), as shown by their respective UV-Vis spectra and ε values (see Experimental Part and Figure S8, ESI). Indeed, the UV-Vis spectrum of complex **5** exhibit a very strong absorption band at λ_{max} = 428 nm (ε = 2 687 $dm^3\ mol^{-1}\ cm^{-1}$) blue shifted and much more intense compared to its Co^{II} analog **3** (λ_{max} = 506 and 529 nm (ε = 0.19 and 0.17 $dm^3\ mol^{-1}\ cm^{-1}$, respectively, Figure S8, ESI). The molecular structure, obtained by an X-ray diffraction study, is depicted in Fig. 3. To the best to our knowledge, only one other compound of the type [Co^{III}(O_2,N_2)(OAc)], with O_2,N_2 = diamino-bis(phenolate) ligand, was structurally characterized [76]. In complex **5**, the Co^{III} metal center is found in a slightly distorted octahedral environment, which is composed of one dianionic κ^4-

(O_2,N_2) diamino-bis(phenolate) ligand and one chelating acetate ligand. Unlike the O3-Co1-O4 angle of 67.41(18)° imposed by the small OAc ligand bite, all other coordination angles around the Co^{III} center are close to the ideal 90° (85.7(2)-95.26(18)°). Interestingly, the bond lengths involving the donor atoms of the supporting ligand **L1** (O1, O2, N1, N2) and the Co^{III} metal center are all slightly shorter than those observed in the analogous [Co^{III}(**L1**)(acac)] complex [56] and in an even more closely related [Co^{III}(O_2,N_2)(OAc)] complex (O_2,N_2 = diamino-bis(phenolate) ligand) that differs only by the substitution of the -CH_2Py arm by a -$CH_2CH_2NMe_2$ arm [76]. However, the Co-O3 and Co-O4 bonds involving the OAc donor atoms are similar to these in the aforementioned related complex reported by Kozak and coll. [76], but significantly longer than those involving the acac group donor atoms of the [Co^{III}(**L1**)(acac)] complex that we recently reported [56].

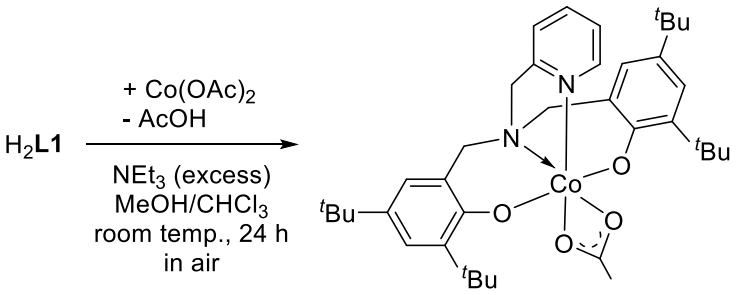

5

Scheme 4. Synthesis of complex **5**.

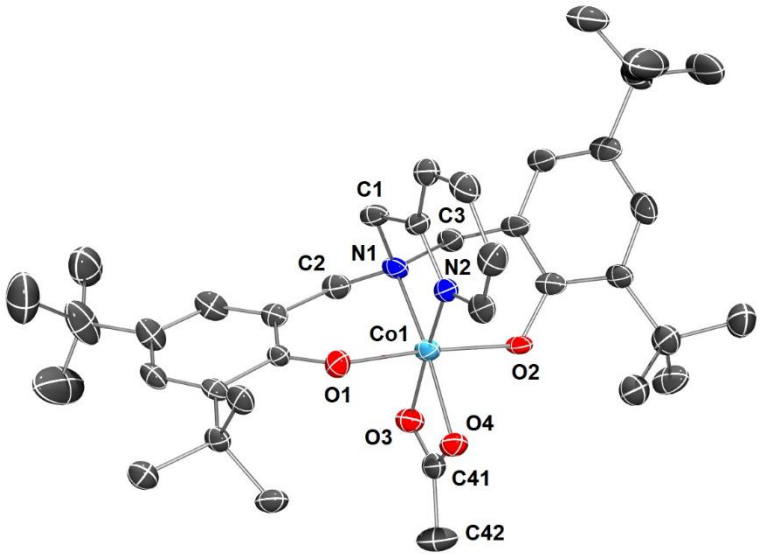

Fig. 3. View of the molecular structure of **5**. The hydrogen atoms are omitted for clarity. Ellipsoids are represented at the 50% probability level. Selected bond lengths (Å) and angles (°): Co1-O1 1.875(4), Co1-O2 1.901(4), Co1-N1 1.942(5), Co1-N2 1.892(5), Co1-O3 1.932(4), Co1-O4 1.970(4), O1-Co1-N1 90.72(18), O1-Co1-N2 85.89(19), O1-Co1-O3 91.14(17), O1-Co1-O4 88.36(17), O2-Co1-N1 95.26(18), O2-Co1-N2 93.96(18), O2-Co1-O3 88.10(17), O2-Co1-O4 85.85(16), N2-Co1-N1 85.7(2), O3-Co1-O4 67.41(18), O4-C41-O3 116.5(6).

Table 1. Crystallographic data for compounds H_2**L1**, **4**·$CHCl_3$ and **5**.

Compound	H_2**L1**	**4**·$CHCl_3$	**5**
CCDC number	2208875	2208876	2208877
Empirical formula	$C_{36}H_{52}N_2O_2$	$C_{27}H_{40}CoN_2O_2$, $CHCl_3$	$C_{38}H_{53}CoN_2O_4$
Formula weight	544.79	602.91	660.75
Temperature, K	173(2)	173(2)	173(2)
Wavelength, Å	1.54184	0.71073	0.71073
Crystal system	Monoclinic	Triclinic	Monoclinic
Space group	P 2_1/c	P -1	C 2/c
a, Å	16.23240(10)	11.1896(4)	29.704(4)
b, Å	8.764	11.8262(6)	17.917(3)
c, Å	23.3993(2)	13.9587(5)	14.5301(19)
α, °	90.0	110.589(2)	90.0
β, °	103.4480(10)	90.937(2)	94.423(4)
γ, °	90.0	118.182(2)	90.0
Volume, Å^3	3237.35(4)	1486.47(11)	7709.7(19)
Z	4	2	8
Density (calc), Mg m^{-3}	1.118	1.347	1.139
Abs. coefficient, mm^{-1}	0.522	0.874	0.482
F(000)	1192	634	2832
Crystal size, mm^3	0.250 x 0.200 x 0.150	0.210 x 0.140 x 0.110	0.100 x 0.080 x 0.020
Theta range, °	2.799 to 71.433	2.117 to 26.368	1.895 to 25,060°
Reflections collected	61043	40512	69569
Indpt reflections (R_{int})	6285 (0.0379)	6074 (0.0371)	6830 (0.2454)
Absorption correction	Multi-scan	Multi-scan	Multi-scan
Max. / min. transmission	1.0 and 0.78295	0.7454 and 0.6903	0.7466 and 0.7156
Refinement method	F^2	F^2	F^2
Data /restraints/parameters	6285 / 0 / 374	6074 / 15 / 321	6830 / 0 / 419
Goodness-of-fit on F^2	1.045	1.026	1.030
R1, wR2 [I>2σ(I)]	0.0416, 0.1088	0.0425, 0.1022	0.0859, 0.1642
R1, wR2 (all data)	0.0443, 0.1118	0.0524, 0.1095	0.1864, 0.2048
Residual density, e Å^{-3}	0.450 / -0.363	0.894 and -0.713	0.948 / -0.501

3.2 Polymerization tests

As stated in the Introduction, our main motivation for carrying this work was to provide new air-, light- and temperature-stable, well-defined unimolecular initiators/moderators for controlled radical polymerization processes. We identified a contribution dating back to the 80's that mentioned the use of a [Co^{III}(salen)(acac)] [Salen = *N*,*N*'-ethylenebis(salicylideneiminato)] complex, which was able to initiate the radical polymerization of methyl methacrylate [78]. The polymerization initiation was proposed to occur *via* the thermal activation of the Co-acac bond (homolysis) and generation of an acac$^{\bullet}$ radical. However, the propagation occurred as in a free-radical mechanism with no indication of a moderating effect by the metal complex, in contrast to a controlled radical polymerization (OMRP). This study inspired our recent work on the development of [Co^{III}(**L1**/**L2**)(acac)] [N_2,O_2 = diamino-bis(phenolate) ligand] for the same purpose. However, these complexes did not show any ability to initiate a radical polymerization [56]. We attributed this lack of reactivity to the (too) strong chelation of the acac ligand, which prevented bond homolysis and departure as a free radical from the Co^{III} center. For this reason, we moved to the synthesis of the analogous OAc complex **5**, OAc supposedly forming a weaker chelate than acac.

Complex **5** was evaluated as initiator for the bulk polymerization of methyl methacrylate (MMA) and methyl acrylate (MA) at 60°C over a period of 24 h and aliquots were withdrawn regularly to monitor the conversion (see Experimental Part). Unfortunately, no polymer formation was observed under these conditions.

While complex **5** was found ineffective as a unimolecular initiator, the potential of its Co^{II} derivative, *i.e*. [Co^{II}(**L1**)] (**3**), to behave as an OMRP moderator *via* reverse initiation remained possible. The bulk polymerization of styrene (St) and *tert*-butyl acrylate (*t*BA) in the presence of **3** or **4** at 65°C using AIBN as radical source (reaction conditions: **3** or **4**/St or *t*BA/AIBN = 1/500/0.6) led to the rapid (few minutes) formation of a hard block of the corresponding polymers, indicating lack of control for these polymerizations. No better control was observed when performing the polymerizations at a lower temperature (30°C) using V-70 as radical initiator. In all cases, the cobalt complexes are fully soluble in the polymerization medium. This behavior is not surprising, since the active radicals of growing polystyrene and polyacrylate chains are known to form weak bonds with certain Co^{II} complexes. Stronger bonds are expected for less-activated monomers. Thus, additional tests were carried out with vinyl acetate (VAc). Indeed, Peng and coll. very recently studied the performances of cobalt complexes of phenoxy-imine ligands towards the radical polymerization of VAc and MA [79]. For certain complexes, the VAc polymerization exhibited the features of controlled chain growth, *i.e*. OMRP, while for other complexes, extensive catalytic chain transfer appeared to take place. As in our case, the polymerization of MA, however, did not show any feature of a controlled process. By analyzing the polymerization results obtained with other four-coordinated cobalt-based systems, the authors concluded that the nature of the coordination geometry (square planar *vs*. tetrahedral) and the spin-state of the Co center were more decisive than the donor atom set (N_4, N_2,O_2, O_4) for the controlled polymerization of both LAMs and MAMs [79, 80]. The results of the bulk polymerization of vinyl acetate under the same conditions, *i.e*. **3**/VAc/AIBN = 1/500/0.6 at 65°C, are presented in Table 2 and GPC traces are available in the ESI (Figure S9). Complex **3** is fully soluble in the polymerization medium under these conditions. Altogether, the fast polymerization rate, rapid formation of a polymeric material with much higher molecular weights ($M_{n(GPC)}$) than expected ($M_{n(theo)}$), which did not evolve much with the conversion, and dispersities between 1.36 and 1.86 imply a lack of control of the radical polymerization process. We observed a similar behavior during the radical polymerization of VAc in the presence of a bis(9-oxyphenalenone) cobalt(II) system, for which the occurrence of catalytic chain transfer (CCT) could be proven [34]. The same polymerization carried out without cobalt complex led to the rapid formation of a highly viscous, nearly solid, mixture (Figure S10 in the ESI). The recorded

data showed that the polymerization was much faster (35% conv in 30 min, vs. 28% in 60 min) and the MW of the PVAc formed much higher (300 000 vs 60 000 g/mol, Figure S10 in the ESI). The data are shown in the SI – Figure S10. As in the case of St and *t*BA, running the polymerization at 30°C, using V-70 as radical initiator, led to slower polymerization rate but did not positively affect the polymerization control. Under the optimized conditions, complex **4** did not perform better than **3**.

Table 2. Bulk polymerization of VAc initiated by AIBN at 65 °C in presence complex **3**.[a]

t (h)	Conv (%)[b]	$M_{n(theo)}$[c]	$M_{n(GPC)}$[d]	$Đ$[d]
0.6	19.7	8400	57 000	1.36
1	28.0	12 040	60 000	1.45
1.5	57.8	24 840	62 000	1.42
2	75.0	32 270	65 000	1.86

[a] Conditions: [**3**]/VAc/AIBN = 1/500/0.6. [b] Measured by ^{1}H NMR. [c] Calculated by conv x 500 x 86.09 (VAc). [d] Measured by GPC in THF (35°C) at a flow of 1 mL/min.

4. Conclusion

We have presented the synthesis and characterization of cobalt(II) (**3**, **4**) and acetato cobalt(III) (**5**) complexes of two tripodal tetradentate diamino-bis(phenolate) ligands (**L1** and **L2**). The solid-state molecular structure of **4** has highlighted the formation of a dimeric structure containing a Co_2O_2 core, in which the cobalt(II) metal ions are five-coordinated in a slightly distorted square planar pyramidal geometry ($\tau = 0.17$). In contrast, the crystal structure of complex **5** revealed, as expected, a monomeric complex in which the cobalt(III) center is six-coordinated, with ligand **L1** acting as a tetradentate dianionic κ^4-(O_2,N_2) chelating ligand and the chelating monoanionic OAc group completing the coordination sphere. The diamagnetic nature of **5** allowed its characterization by multinuclear NMR spectroscopic techniques. Complex **5** was evaluated as unimolecular initiator for the radical polymerization of MA nor MMA without success. The potential of its cobalt(II) analog (**3**) to moderate the radical polymerization of activated (St, *t*BA) or non-activated (VAc) monomers was also evaluated, and no features of a controlled polymerization process could be recorded. From this study and from our previous work on acetylacetonato cobalt(III) complexes of diamino-bis(phenolate) ligands [56], it clearly appears that the combination of this ligand scaffold and cobalt is not best suited for the targeted application. We are therefore exploring other ligand architectures to develop original air-, light- and thermally stable unimolecular initiators of radical polymerization processes.

Conflict of interest

The authors declare no conflict of interest.

Acknowledgements

The authors thank the Agence Nationale de la Recherche, France (Grant ANR-19-CE07-0031-01, POLYSWITCH) for support of this work. Additional support by the Ministère de l'Enseignement Supérieur et de la Recherche Scientifique, France (PROFAS B+ fellowship to Y.K.R), the Centre National de la Recherche Scientifique (CNRS, France) and the Institut Universitaire de France (IUF, France) are also gratefully acknowledged.

Supplementary data

ESI-MS spectra of complexes **3**-**5**; NMR spectra of complex **5**; UV-Vis spectra of complexes **3**-**5**; GPC traces of the bulk polymerization of VAc initiated by AIBN at 65 °C in presence or absence of complex **3** are available in the Electronic Supporting Information. CCDC 2208875 (H_2**L1**), 2208876 (**4**·$CHCl_3$) and 2208877 (**5**) contain the supplementary crystallographic data for this paper. These data are provided free of charge by the Cambridge Crystallographic Data Centre. Supplementary data to this article can be found online at https://doi.org/xxx.

References

[1] D. Hernández-Romero, S. Rosete-Luna, A. López-Monteon, A. Chávez-Piña, N. Pérez-Hernández, J. Marroquín-Flores, A. Cruz-Navarro, G. Pesado-Gómez, D. Morales-Morales, R. Colorado-Peralta, First-row transition metal compounds containing benzimidazole ligands: An overview of their anticancer and antitumor activity, Coord. Chem. Rev., 439 (2021) 213930. 10.1016/j.ccr.2021.213930.

[2] A.K. Renfrew, E.S. O'Neill, T.W. Hambley, E.J. New, Harnessing the properties of cobalt coordination complexes for biological application, Coord. Chem. Rev., 375 (2018) 221-233. 10.1016/j.ccr.2017.11.027.

[3] E.L. Chang, C. Simmers, D.A. Knight, Cobalt Complexes as Antiviral and Antibacterial Agents, Pharmaceuticals, 2010, pp. 1711-1728.

[4] Y. Rechkemmer, F.D. Breitgoff, M. van der Meer, M. Atanasov, M. Hakl, M. Orlita, P. Neugebauer, F. Neese, B. Sarkar, J. van Slageren, A four-coordinate cobalt(II) single-ion magnet with coercivity and a very high energy barrier, Nat. Commun., 7 (2016) 10467. 10.1038/ncomms10467.

[5] M. Murrie, Cobalt(ii) single-molecule magnets, Chem. Soc. Rev., 39 (2010) 1986-1995. 10.1039/B913279C.

[6] M. Li, J. Lu, Cobalt in lithium-ion batteries, Science, 367 (2020) 979-980. 10.1126/science.aba9168.

[7] S.S. Bera, M. Szostak, Cobalt–N-Heterocyclic Carbene Complexes in Catalysis, ACS Catal., 12 (2022) 3111-3137. 10.1021/acscatal.1c05869.

[8] D. Xiao, J. Gregg, K.V. Lakshmi, P.J. Bonitatibus, Bio-Inspired Molecular Catalysts for Water Oxidation, Catalysts, 2021.

[9] R. Matheu, P. Garrido-Barros, M. Gil-Sepulcre, M.Z. Ertem, X. Sala, C. Gimbert-Suriñach, A. Llobet, The development of molecular water oxidation catalysts, Nat. Rev. Chem., 3 (2019) 331-341. 10.1038/s41570-019-0096-0.

[10] K. Junge, V. Papa, M. Beller, Cobalt–Pincer Complexes in Catalysis, Chem. Eur. J., 25 (2019) 122-143. 10.1002/chem.201803016.

[11] W. Liu, B. Sahoo, K. Junge, M. Beller, Cobalt Complexes as an Emerging Class of Catalysts for Homogeneous Hydrogenations, Acc. Chem. Res., 51 (2018) 1858-1869. 10.1021/acs.accounts.8b00262.

[12] A.M. Anderson-Wile, J.B. Edson, G.W. Coates, 3.23 - Living Transition Metal-Catalyzed Alkene Polymerization: Polyolefin Synthesis and New Polymer Architectures, in: K. Matyjaszewski, M. Möller (Eds.) Polymer Science: A Comprehensive Reference, Elsevier, Amsterdam, 2012, pp. 739-778.

[13] C. Fliedel, S. Dagorne, E. Le Roux, 9.14 - Metal Complexes as Catalysts/Moderators for Polymerization Reactions, in: E.C. Constable, G. Parkin, L. Que Jr (Eds.) Comprehensive Coordination Chemistry III, Elsevier, Oxford, 2021, pp. 410-464.

[14] C.M. Kozak, K. Ambrose, T.S. Anderson, Copolymerization of carbon dioxide and epoxides by metal coordination complexes, Coord. Chem. Rev., 376 (2018) 565-587. 10.1016/j.ccr.2018.08.019.

[15] H. Ajiro, P.C.B. Widger, S.M. Ahmed, S.D. Allen, G.W. Coates, 4.09 - Stereoselective Ring-Opening Polymerization of Epoxides, in: K. Matyjaszewski, M. Möller (Eds.) Polymer Science: A Comprehensive Reference, Elsevier, Amsterdam, 2012, pp. 165-181.

[16] C. Fliedel, R. Poli, Homolytically weak metal-carbon bonds make robust controlled radical polymerizations systems for "less-activated monomers", J. Organomet. Chem., 880 (2019) 241-252. 10.1016/j.jorganchem.2018.11.012.
[17] A. Debuigne, C. Jérôme, C. Detrembleur, Organometallic-mediated radical polymerization of 'less activated monomers': Fundamentals, challenges and opportunities, Polymer, 115 (2017) 285-307. 10.1016/j.polymer.2017.01.008.
[18] R. Poli, Organometallic Mediated Radical Polymerization, in: K. Matyjaszewski, M. Möller (Eds.) Polymer Science: A Comprehensive Reference, Elsevier BV, Amsterdam, 2012, pp. 351-375.
[19] M. Hurtgen, C. Detrembleur, C. Jerome, A. Debuigne, Insight into Organometallic-Mediated Radical Polymerization, Polym. Rev., 51 (2011) 188-213. 10.1080/15583724.2011.566401.
[20] A. Debuigne, R. Poli, C. Jerome, R. Jerome, C. Detrembleur, Overview of cobalt-mediated radical polymerization: Roots, state of the art and future prospects, Prog. Polym. Sci., 34 (2009) 211-239. 10.1016/j.progpolymsci.2008.11.003.
[21] R. Poli, Relationship between one-electron transition-metal reactivity and radical polymerization processes, Angew. Chem. Int. Ed., 45 (2006) 5058-5070. 10.1002/anie.200503785.
[22] C.H. Peng, T.Y. Yang, Y. Zhao, X. Fu, Reversible deactivation radical polymerization mediated by cobalt complexes: recent progress and perspectives, Org. Biomol. Chem., 12 (2014) 8580-8587. 10.1039/c4ob01427h.
[23] M.R. Kember, A. Buchard, C.K. Williams, Catalysts for CO2/epoxide copolymerisation, Chem. Commun., 47 (2011) 141-163. 10.1039/C0CC02207A.
[24] D.J. Darensbourg, Making Plastics from Carbon Dioxide: Salen Metal Complexes as Catalysts for the Production of Polycarbonates from Epoxides and CO2, Chem. Rev., 107 (2007) 2388-2410. 10.1021/cr068363q.
[25] K. Ambrose, K.N. Robertson, C.M. Kozak, Cobalt amino-bis(phenolate) complexes for coupling and copolymerization of epoxides with carbon dioxide, Dalton Trans., 48 (2019) 6248-6260. 10.1039/C9DT00996E.
[26] M. Reiter, P.T. Altenbuchner, S. Kissling, E. Herdtweck, B. Rieger, Amine-bis(phenolato)cobalt(II) Catalysts for the Formation of Organic Carbonates from Carbon Dioxide and Epoxides, Eur. J. Inorg. Chem., 2015 (2015) 1766-1774. 10.1002/ejic.201403087.
[27] M.R. Kember, F. Jutz, A. Buchard, A.J.P. White, C.K. Williams, Di-cobalt(ii) catalysts for the copolymerisation of CO2 and cyclohexene oxide: support for a dinuclear mechanism?, Chem. Sci., 3 (2012) 1245-1255. 10.1039/C2SC00802E.
[28] K. Matyjaszewski, J. Xia, Atom Transfer Radical Polymerization, Chem. Rev., 101 (2001) 2921-2990.
[29] T.G. Ribelli, M. Fantin, J.C. Daran, K.F. Augustine, R. Poli, K. Matyjaszewski, Synthesis and Characterization of the Most Active Copper ATRP Catalyst Based on Tris[(4-dimethylaminopyridyl)methyl]amine, J. Am. Chem. Soc., 140 (2018) 1525-1534. 10.1021/jacs.7b12180.
[30] R. Poli, Radical Coordination Chemistry and Its Relevance to Metal-Mediated Radical Polymerization, Eur. J. Inorg. Chem., (2011) 1513-1530. 10.1002/ejic.201001364.
[31] L. Thevenin, C. Fliedel, K. Matyjaszewski, R. Poli, Impact of Catalyzed Radical Termination (CRT) and Reductive Radical Termination (RRT) in Metal-Mediated Radical Polymerization Processes, Eur. J. Inorg. Chem., 2019 (2019) 4489-4499. 10.1002/ejic.201900901.
[32] M. Fantin, F. Lorandi, T.G. Ribelli, G. Szczepaniak, A.E. Enciso, C. Fliedel, L. Thevenin, A.A. Isse, R. Poli, K. Matyjaszewski, Impact of Organometallic Intermediates on Copper-Catalyzed Atom Transfer Radical Polymerization, Macromolecules, 52 (2019) 4079-4090. 10.1021/acs.macromol.9b00870.
[33] L. Thevenin, C. Fliedel, M. Fantin, T.G. Ribelli, K. Matyjaszewski, R. Poli, Reductive Termination of Cyanoisopropyl Radicals by Copper(I) Complexes and Proton Donors: Organometallic Intermediates or Coupled Proton-Electron Transfer?, Inorg. Chem., 58 (2019) 6445-6457. 10.1021/acs.inorgchem.9b00660.

[34] E.V. Bellan, L. Thevenin, F. Gayet, C. Fliedel, R. Poli, Catalyzed Chain Transfer in Vinyl Acetate Polymerization Mediated by 9-Oxyphenalenone Cobalt(II) Complexes, Acs Macro Letters, 6 (2017) 959-962. 10.1021/acsmacrolett.7b00551.
[35] T.G. Ribelli, S.M. Wahidur Rahaman, J.-C. Daran, P. Krys, K. Matyjaszewski, R. Poli, Effect of Ligand Structure on the CuII–R OMRP Dormant Species and Its Consequences for Catalytic Radical Termination in ATRP, Macromolecules, 49 (2016) 7749-7757. 10.1021/acs.macromol.6b01334.
[36] R. Poli, New Phenomena in Organometallic-Mediated Radical Polymerization (OMRP) and Perspectives for Control of Less Active Monomers, Chem. Eur. J., 21 (2015) 6988-7001. 10.1002/chem.201500015.
[37] N. Corrigan, K. Jung, G. Moad, C.J. Hawker, K. Matyjaszewski, C. Boyer, Reversible-deactivation radical polymerization (Controlled/living radical polymerization): From discovery to materials design and applications, Prog. Polym. Sci., 111 (2020) 101311. 10.1016/j.progpolymsci.2020.101311.
[38] A.D. Jenkins, R.G. Jones, G. Moad, Terminology for reversible-deactivation radical polymerization previously called "controlled" radical or "living" radical polymerization (IUPAC Recommendations 2010), Pure Appl. Chem., 82 (2010) 483-491. doi:10.1351/PAC-REP-08-04-03.
[39] M. Destarac, Industrial development of reversible-deactivation radical polymerization: is the induction period over?, Polym. Chem., 9 (2018) 4947-4967. 10.1039/c8py00970h.
[40] M. Destarac, Controlled Radical Polymerization: Industrial Stakes, Obstacles and Achievements, Macromol. React. Engin., 4 (2010) 165-179. 10.1002/mren.200900087.
[41] K. Matyjaszewski, Advanced Materials by Atom Transfer Radical Polymerization, Adv. Mater., 30 (2018) e1706441. 10.1002/adma.201706441.
[42] T.G. Ribelli, F. Lorandi, M. Fantin, K. Matyjaszewski, Atom Transfer Radical Polymerization: Billion Times More Active Catalysts and New Initiation Systems, Macromol. Rapid Commun., 40 (2019) e1800616. 10.1002/marc.201800616.
[43] X. Pan, M. Fantin, F. Yuan, K. Matyjaszewski, Externally controlled atom transfer radical polymerization, Chem. Soc. Rev., 47 (2018) 5457-5490. 10.1039/c8cs00259b.
[44] A. Debuigne, J.R. Caille, R. Jerome, Highly efficient cobalt-mediated radical polymerization of vinyl acetate, Angew. Chem. Int. Ed., 44 (2005) 1101-1104. 10.1002/anie.200461333.
[45] Y. Piette, A. Debuigne, V. Bodart, N. Willet, A.S. Duwez, C. Jerome, C. Detrembleur, Synthesis of poly(vinyl acetate)-b-poly(vinyl chloride) block copolymers by Cobalt-Mediated Radical Polymerization (CMRP), Polym. Chem., 4 (2013) 1685-1693. 10.1039/c2py20965a.
[46] S. Banerjee, V. Ladmiral, A. Debuigne, C. Detrembleur, R. Poli, B.M. Ameduri, Organometallic-Mediated Radical Polymerization of Vinylidene Fluoride, Angew. Chem. Int. Ed., 57 (2018) 2934-2937. 10.1002/anie.201712347.
[47] M. Michelas, C. Fliedel, R. Poli, 1.03 - Reversible Homolysis of Metal-Carbon Bonds, in: G. Parkin, K. Meyer, D. O'hare (Eds.) Comprehensive Organometallic Chemistry IV, Elsevier, Oxford, 2022, pp. 31-85.
[48] J. Demarteau, A. Debuigne, C. Detrembleur, Organocobalt Complexes as Sources of Carbon-Centered Radicals for Organic and Polymer Chemistries, Chem. Rev., 119 (2019) 6906-6955. 10.1021/acs.chemrev.8b00715.
[49] J. Demarteau, A. Kermagoret, I. German, D. Cordella, K. Robeyns, J. De Winter, P. Gerbaux, C. Jérôme, A. Debuigne, C. Detrembleur, Halomethyl-cobalt(bis-acetylacetonate) for the controlled synthesis of functional polymers, Chem. Commun., 51 (2015) 14334-14337. 10.1039/c5cc04714e.
[50] Y. Zhao, M. Yu, S. Zhang, Z. Wu, Y. Liu, C.H. Peng, X. Fu, A well-defined, versatile photoinitiator (salen)Co-CO2CH3 for visible light-initiated living/controlled radical polymerization, Chem. Sci., 6 (2015) 2979-2988. 10.1039/c5sc00477b.
[51] A. Debuigne, Y. Champouret, R. Jerome, R. Poli, C. Detrembleur, Mechanistic insights into the cobalt-mediated radical polymerization (CMRP) of vinyl acetate with cobalt(III) adducts as initiators, Chem. Eur. J., 14 (2008) 4046-4059. 10.1002/chem.200701867.
[52] R. Morales-Cerrada, V. Ladmiral, F. Gayet, C. Fliedel, R. Poli, B. Ameduri, Fluoroalkyl Pentacarbonylmanganese(I) Complexes as Initiators for the Radical (co)Polymerization of Fluoromonomers, Polymers, 12 (2020). 10.3390/polym12020384.

[53] R. Morales-Cerrada, C. Fliedel, J.C. Daran, F. Gayet, V. Ladmiral, B. Ameduri, R. Poli, Fluoroalkyl Radical Generation by Homolytic Bond Dissociation in Pentacarbonylmanganese Derivatives, Chemistry-a European Journal, 25 (2019) 296-308. 10.1002/chem.201804007.
[54] L.E.N. Allan, J.P. MacDonald, A.M. Reckling, C.M. Kozak, M.P. Shaver, Controlled Radical Polymerization Mediated by Amine-Bis(phenolate) Iron(III) Complexes, Macromol. Rapid Commun., 33 (2012) 414-418. 10.1002/marc.201100872.
[55] Y. Shimazaki, S. Huth, A. Odani, O. Yamauchi, A structural model for the galactose oxidase active site which shows counteranion-dependent phenoxyl radical formation by disproportionation, Angew. Chem. Int. Ed., 39 (2000) 1666-1669.
[56] Y.K. Redjel, L. Thevenin, J.C. Daran, M. Benslimane, R. Poli, C. Fliedel, Acetylacetonato cobalt(III) and iron(III) complexes of picolylamine- and aminopropylamine-bis(phenolate) ligands: Synthesis, characterization and crystal structures, Polyhedron, 158 (2019) 83-90. 10.1016/j.poly.2018.09.021.
[57] G.M. Sheldrick, Acta Crystallogr. Sect. A: Found. Crystallogr., A71 (2015) 3-8.
[58] G.M. Sheldrick, Acta Crystallogr. Sect. C: Cryst. Struct. Commun., C71 (2015) 3-8.
[59] A.L. Spek, J. Appl. Crystallogr., 36 (2003) 7-13.
[60] N. Takayuki, I. Shinobu, Catalytic Alkane Hydroxylation Reaction with Nickel(II) Complexes Supported by Di- and Triphenol Ligands, Chem. Lett., 36 (2007) 748-749. 10.1246/cl.2007.748.
[61] A.K. Bowser, A.M. Anderson-Wile, D.H. Johnston, B.M. Wile, Diamine bis(phenolate) and pendant amine bis(phenolate) ligands: catalytic activity for the room temperature palladium-catalyzed Suzuki-Miyauracoupling reaction, Appl. Organomet. Chem., 30 (2016) 32-39. 10.1002/aoc.3396.
[62] M. Taherimehr, J.P. Serta, A.W. Kleij, C.J. Whiteoak, P.P. Pescarmona, New iron pyridylamino-bis(phenolate) catalyst for converting CO2 into cyclic carbonates and cross-linked polycarbonates, ChemSusChem, 8 (2015) 1034-1042. 10.1002/cssc.201403323.
[63] H. Schroeder, B.R.M. Lake, S. Demeshko, M.P. Shaver, M. Buback, A Synthetic and Multispectroscopic Speciation Analysis of Controlled Radical Polymerization Mediated by Amine–Bis(phenolate)iron Complexes, Macromolecules, 48 (2015) 4329-4338. 10.1021/acs.macromol.5b01175.
[64] Y. Chapurina, J. Klitzke, L. Casagrande Ode, Jr., M. Awada, V. Dorcet, E. Kirillov, J.F. Carpentier, Scandium versus yttrium{amino-alkoxy-bis(phenolate)} complexes for the stereoselective ring-opening polymerization of racemic lactide and beta-butyrolactone, Dalton Trans., 43 (2014) 14322-14333. 10.1039/c4dt01206b.
[65] O. Wichmann, K. Ahonen, R. Sillanpää, Uranyl(VI) complexes with a diaminobisphenol from eugenol and N-(2-aminoethyl)morpholine: Syntheses, structures and extraction studies, Polyhedron, 30 (2011) 477-485. 10.1016/j.poly.2010.11.012.
[66] R. Poli, L.E.N. Allan, M.P. Shaver, Iron-mediated reversible deactivation controlled radical polymerization, Prog. Polym. Sci., 39 (2014) 1827-1845. 10.1016/j.progpolymsci.2014.06.003.
[67] L. Thevenin, J.C. Daran, R. Poli, C. Fliedel, Cobalt complexes of an OSNSO-tetrapodal pentadentate ligand: Synthesis, structures and reactivity, Inorganica Chimica Acta, 518 (2021). 10.1016/j.ica.2020.120215.
[68] A.W. Addison, T.N. Rao, J. Reedijk, J. van Rijn, G.C. Verschoor, Synthesis, structure, and spectroscopic properties of copper(II) compounds containing nitrogen–sulphur donor ligands; the crystal and molecular structure of aqua[1,7-bis(N-methylbenzimidazol-2'-yl)-2,6-dithiaheptane]copper(II) perchlorate, J. Chem. Soc., Dalton Trans., (1984) 1349-1356. 10.1039/DT9840001349.
[69] The τ value is accessible through the relation τ = (β - α)/60, where α and β are the angles that are opposite each other in the plane (e.g. N_2O_2 for Salen ligands), and by convention β is the most obtuse angle. The τ value ranges from 0 to 1; a value of 0 identifies a perfectly SP geometry and a value of 1 a perfectly TBP.
[70] A. Mukherjee, F. Lloret, R. Mukherjee, Diphenoxido-Bridged CoII and ZnII Complexes of Tripodal N2O2 Ligands: Stabilisation of MII-Coordinated Phenoxyl Radical Species, Eur. J. Inorg. Chem., 2010 (2010) 1032-1042. 10.1002/ejic.200900760.

[71] E. Labisbal, L. Rodríguez, O. Souto, A. Sousa-Pedrares, J.A. García-Vázquez, J. Romero, A. Sousa, M. Yáñez, F. Orallo, J.A. Real, Electrochemical synthesis and structural characterization of Co(II), Ni(II) and Cu(II) complexes of N,N-bis(4,5-dimethyl-2-hydroxybenzyl)-N-(2-pyridylmethyl)amine, Dalton Trans., (2009) 8644-8656. 10.1039/B907539A.
[72] A. Mukherjee, F. Lloret, R. Mukherjee, Synthesis and Properties of Diphenoxo-Bridged CoII, NiII, CuII, and ZnII Complexes of a New Tripodal Ligand: Generation and Properties of MII-Coordinated Phenoxyl Radical Species, Inorg. Chem., 47 (2008) 4471-4480. 10.1021/ic701283b.
[73] D. Schnieders, A. Hammerschmidt, M. Merkel, F. Schweppe, B. Krebs, Zinc and Cobalt Complexes Derived from Tetradentate Tripodal Ligands with N2O2 Donorset as Model Compounds for Phosphatases, Z. Anorg. Allg. Chem., 634 (2008) 2933-2939. 10.1002/zaac.200800390.
[74] L. Rodríguez, E. Labisbal, A. Sousa-Pedrares, J.A. García-Vázquez, J. Romero, M.L. Durán, J.A. Real, A. Sousa, Coordination Chemistry of Amine Bis(phenolate) Cobalt(II), Nickel(II), and Copper(II) Complexes, Inorg. Chem., 45 (2006) 7903-7914. 10.1021/ic0602594.
[75] U.K. Das, J. Bobak, C. Fowler, S.E. Hann, C.F. Petten, L.N. Dawe, A. Decken, F.M. Kerton, C.M. Kozak, Synthesis and structure of mono-, bi- and trimetallic amine-bis(phenolate) cobalt(II) complexes, Dalton Trans., 39 (2010) 5462-5477. 10.1039/c002843f.
[76] L.N. Saunders, M.E. Pratt, S.E. Hann, L.N. Dawe, A. Decken, F.M. Kerton, C.M. Kozak, Structural variations in the coordination chemistry of amine-bis(phenolate) cobalt(II/III) complexes, Polyhedron, 46 (2012) 53-65. 10.1016/j.poly.2012.07.082.
[77] A. Garai, I. Pant, S. Banerjee, B. Banik, P. Kondaiah, A.R. Chakravarty, Photorelease and Cellular Delivery of Mitocurcumin from Its Cytotoxic Cobalt(III) Complex in Visible Light, Inorg. Chem., 55 (2016) 6027-6035. 10.1021/acs.inorgchem.6b00554.
[78] R. Thiagarajan, V. Kalpagam, U.S. Nandi, Mixed ligand complexes in vinyl polymerization. I. [N,N'-ethylenebis (salicylideneiminato)](acetylacetonato)cobalt(III) as an initiator, J. Polym. Sci. A Polym. Chem., 20 (1982) 675-681. 10.1002/pol.1982.170200308.
[79] Y.-H. Chen, S.-J. Chen, J.-Q. Li, Z. Wu, G.-H. Lee, Y.-H. Liu, W.-T. Cheng, C.-Y. Yeh, C.-H. Peng, Cobalt(II) phenoxy-imine complexes in radical polymerization of vinyl acetate: The interplay of catalytic chain transfer and controlled/living radical polymerization, J. Polym. Sci., 58 (2020) 101-113. 10.1002/pola.29460.
[80] W. Benchaphanthawee, C.-H. Peng, Organo-Cobalt Complexes in Reversible-Deactivation Radical Polymerization, Chem. Rec., 21 (2021) 3628-3647. 10.1002/tcr.202100122.